

Research Article

Identification and Analysis of Crucial Genes in *H. pylori*-Associated Gastric Cancer Using an Integrated Bioinformatics Approach

Wei Ding ^{1,2,3}, Huaji Jiang,^{1,2} Nianyuan Ye,^{1,2} Ling Zhuang,^{1,2} Zhiping Yuan,⁴ Yulin Tan ^{1,2}, Wenbo Xue ^{1,2} and Xuezhong Xu ^{1,2}

¹Department of General Surgery, Wujin Hospital Affiliated to Jiangsu University, Changzhou 213017, China

²Department of General Surgery, The Wujin Clinical College of Xuzhou Medical University, Changzhou 213017, China

³Changzhou Key Laboratory of Molecular Diagnostics and Precision Cancer Medicine, Changzhou 213017, China

⁴Department of Gastroenterology, Wujin Hospital Affiliated with Jiangsu University, Changzhou 213017, China

Correspondence should be addressed to Yulin Tan; tanyldoctor@163.com, Wenbo Xue; xwbdoctor@163.com, and Xuezhong Xu; xxzdoctor@163.com

Received 2 September 2022; Revised 25 September 2022; Accepted 25 November 2022; Published 1 February 2023

Academic Editor: Yanqing Liu

Copyright © 2023 Wei Ding et al. This is an open access article distributed under the Creative Commons Attribution License, which permits unrestricted use, distribution, and reproduction in any medium, provided the original work is properly cited.

Background. The relationship between *H. pylori* infection and gastric cancer (GC) has been widely studied, and *H. pylori* is considered as the main factor. Utilizing bioinformatics analysis, this study examined gene signatures related to progressing *H. pylori*-associated GC. **Materials and Methods.** The dataset GSE13195 was chosen to search for abnormally expressed genes in *H. pylori*-associated GC and normal tissues. The TCGA-STAD database was chosen to verify the expression of key genes in GC and normal tissues. **Results.** In GSE13195, a total of 332 differential expression genes (DEGs) were screened. The results of weighted gene co-expression network analysis showed that the light cyan, plum2, black, and magenta4 modules were associated with stages (T3, T2, and T4), while the orangered4, salmon2, pink, and navajowhite2 modules were correlated with lymph node metastasis (N3, N2, and N0). Based on the results of DEGs and hub genes, a total of 7 key genes (ADAM28, FCER1G, MRPL14, SOSTDC1, TYROBP, C1QC, and C3) were screened out. These gene mRNA levels were able to distinguish between normal and *H. pylori*-associated GC tissue using receiver operating characteristic curves. After transcriptional level verification and survival analysis, ADAM28 and C1QC were excluded. An immune infiltration study revealed that key genes were involved in regulating the infiltration levels of cells associated with innate immune response, antigen presentation process, humoral immune response, or Tcell-mediated immune response. In addition, drugs targeting FCER1G and TYROBP have been approved and are under investigation. **Conclusion.** Our study identified five key genes involved in *H. pylori*-associated GC tumorigenesis. Patients with higher levels of C3 expression had a poorer prognosis than those with lower levels. In addition, these key genes may serve as biomarkers and therapeutic targets for *H. pylori*-associated GC diagnosis, targeted therapy, and immunotherapy in the future.

1. Introduction

Incidence of gastric cancer (GC) is the sixth highest of all cancer types, with approximately 1,089,103 cases worldwide. GC is also the third leading cause of cancer death, with approximately 769,000 deaths each year [1]. The number of new cases of GC in China approaches 0.5 million each year [2]. Currently, the 5-year survival rate of GC patients is 32%, and more than 50% of patients are diagnosed with advanced

cancer [3]. So far, surgery remains the only cure for GC [4]. The Human Genome Project is nearing completion and next-generation sequencing is being widely applied; researchers have made great progress in the study of the mechanism of GC occurrence and development [5]. The new medical model of the cross-development of sequencing technology and bioinformatics utilizes genomics and proteomics to guide targeted therapy, enabling GC patients to receive individualized and precise treatment [6]. To decrease

the high incidence and mortality of GC, early detection and diagnosis are urgently needed, as well as new biomarkers for the disease. Although technology has advanced considerably, there is still an urgent need for efficient and timely diagnostic methods and new GC-specific biomarkers.

Various risk factors affect the incidence of GC, including *Helicobacter pylori* (*H. pylori*) infection, gender, poor dietary habits, and smoking [7]. Of these, *H. pylori* infection, which often leads to gastritis, followed by gastric atrophy and gastrointestinal metaplasia, is most closely related to GC [8]. Currently, the detection of *H. pylori* and its eradication therapy can reduce the risk of GC [9]. Mechanistically, the toxic effects of *H. pylori*-produced cytotoxicity-associated gene A (CagA) and vacuolar cytotoxicity A (VacA) proteins on gastric mucosal cells can trigger a series of complex biological effects, including release of proinflammatory cytokines, recruitment of immune cells, and stimulation of the survival of gastric epithelial cells [10, 11]. *H. pylori* inhibits phagocytic activity and T cell function during infection, while catalyzing the formation of urea to ensure its survival in harsh low pH conditions. Furthermore, *H. pylori* metabolism byproducts damage epithelial cells of the host and contribute to the carcinogenesis of *H. pylori* infection [12]. Despite numerous studies on *H. pylori*, it remains unclear whether *H. pylori* is only involved in the initiation of gastric tumor processes, or whether it affects the mechanisms of tumor progression.

In recent years, immunotherapy, as a novel treatment method, mainly induces antitumor effects by modulating the immune system and has made revolutionary progress in the treatment of gastric cancer [13]. The tumor microenvironment (TME) is a complex ecosystem consisting of immune cells coming in many forms and other acellular components of the extracellular matrix with marked heterogeneity. In the TME, tumor cells and immunomodulators interact dynamically to produce positive immunotherapy responses [14]. The immune microenvironment of GC itself is in a dynamic change, and whether the addition of *H. pylori* will make it more complicated.

In this article, based on the GSE13195 dataset and the TCGA-STAD dataset, we used a series of bioinformatics research methods to explore the dysregulated genes and mechanisms in *H. pylori*-associated GC tissues and to find possible biomarkers and targeted drugs.

2. Materials and Methods

2.1. Data Collection and Analysis. We selected the dataset GSE13195 from the Gene Expression Omnibus (GEO, <https://www.ncbi.nlm.nih.gov/geo/>) for our study [15]. The dataset was derived from GPL5175 (Affymetrix Human Exon 1.0 ST Array) and contained *H. pylori*-associated GC and normal tissues from 25 patients. The dataset also included patients' pathological information, tumor stages (T2, T3, and T4), and lymph node metastasis (N0, N2, and N3). Subsequently, Sangerbox Tools (<https://www.sangerbox.com/>) were used for normalized raw data as well as

multiarray analysis ("lima" package) [16]. Finally, 134 downregulated genes and 198 upregulated genes were obtained according to the screening conditions of P value <0.05 and $|\log_{2}FC| > 1$.

2.2. Functional and Pathway Enrichment Analysis. Genes differentially expressed were functionally enriched using DAVID v6.8 (Database of Annotations, Visualization, and Integrated Discovery, <https://david.ncicrf.gov/home.jsp>) [17]. These include Gene Ontology (GO) enrichment analysis and Kyoto Encyclopedia of Genes and Genomes (KEGG) pathway analysis.

2.3. Gene Set Enrichment Analysis (GSEA). To more accurately determine the functions of differential genes, we performed GSEA using Sangerbox Tools on the basis of normal tissues and *H. pylori*-associated GC tissues [16]. The reference gene set is *c2.cp.kegg.v7.0*.

2.4. Screen for Tumor Progression-Related Modules and Central Genes by Weighted Gene Co-Expression Network Analysis (WGCNA). Gene co-expression networks in *H. pylori*-associated GC tissues were constructed using Sangerbox Tools [16]. First, based on Pearson correlation analysis, 25 samples were clustered to identify outliers. Then, we set the soft threshold to 5 to achieve a scale-free topology. Subsequently, using a dynamic tree-cut approach, the genes were classified into different modules based on gene expression correlations. The expression similarity of module eigen genes was further used to cluster similar modules with a height of 0.85. Module membership (MM) is the correlation of gene expression profiles with module characteristic genes, and genes with $MM \geq 0.8$ are considered hub genes [18]. The protein interaction network was mapped using the String online website (<https://string-db.org/>).

2.5. Validation of Key Genes. Key genes were selected from abnormally expressed genes and hub genes. Receiver operating characteristic (ROC) curves were drawn to calculate specificity and sensitivity. In order to verify the accuracy and reliability of the screened key genes, the gene expression data of GC patients in the TCGA-STAD dataset (including 34 normal samples, 20 *H. pylori*-associated GC samples, 157 *H. pylori*-unassociated GC samples, and 153 other samples) were used for validation (including mRNA expression level and survival analysis) in UALCAN online website (<https://ualcan.path.uab.edu/>) [19].

2.6. Immune Infiltration Analysis. According to the calculation method of the immune microenvironment score of CIBERSORT, the immune microenvironment analysis of *H. pylori*-associated GC tissues and normal tissues was performed [20]. We calculated enrichment scores for each immune-related cell population using ssGSEA to examine the relationship between key genes and immune infiltration. In addition, Spearman correlations between each hub gene expression and immune enrichment scores were calculated and tested.

2.7. Target Drug. The DrugBank online analysis website (<https://go.drugbank.com/>) was used to find compounds that might act on key genes [21]. The flowchart of the study is provided in Figure 1.

3. Results

3.1. Data Collection and Acquisition of Differential Genes. The dataset GSE13195 from GEO was selected for this study. According to the screening conditions of $P < 0.05$ and $|\log_{2}FC| > 1$, we found 332 differentially expressed genes (DEGs), including 198 that were upregulated and 134 that were downregulated (Figures 2(a) and 2(b)).

3.2. Functional and Pathway Enrichment Analysis. DAVID v6.8 was used for GO and KEGG enrichment analysis in order to better elucidate the functional and biological significance of the modules identified. GO biological process analysis showed that in terms of biological process, these differential genes were mainly related with cell adhesion, collagen fibril organization, response to drug, maintenance of gastrointestinal epithelium and detoxification of copper ion; in terms of cellular components, these differential genes were mainly located in extracellular space, extracellular exosome, extracellular region, cell surface, and basolateral plasm membrane; in terms of molecular functions, these differential genes mainly participated in extracellular matrix structural constituent, identical protein binding, protein binding, integrin binding, and collagen binding (Figure 2(c)). Furthermore, KEGG analysis revealed that these differential genes were highly involved in the regulation of gastric acid secretion, mineral absorption, protein digestion and absorption, ECM-receptor interaction, and cell cycle (Figure 2(d)).

3.3. Differential Gene Set Enrichment Analysis. GSEA was conducted to better elucidate how differential genes function. The eight KEGG pathways associated with DEGs are shown in Figure 2(e). They were melanogenesis, thyroid cancer, bladder cancer, P53 signaling pathway, glycosphingolipid biosynthesis, renal cell carcinoma, basal cell carcinoma, and endometrial cancer. Moreover, compared with normal tissues, these related pathways were hyperactivated in *H. pylori*-associated GC tissues.

3.4. Co-Expression Network Construction and Module Detection. To find modules highly correlated with the progression of *H. pylori*-associated GC, samples of cancer tissues were used to construct a network of co-expression. We investigated the relationship between the scale-free topological fit index R^2 and the soft threshold (power) in order to make the network scale-free. As shown in Figures 3(a) and 3(b), we chose a soft threshold (power) of 5 when R^2 reached 0.85 for the first time. After the adjacency matrix was constructed, we transformed it into a topological overlap matrix. Genes were then sorted into different modules, performing a dynamic tree-cutting method.

Different genes would be categorized into the same module if their expressions were significantly correlated. Finally, we got 66 modules; the module feature vector and clustering dendrogram are shown in Figures 3(c) and 3(d). Then, to identify modules that were highly correlated with the progression of *H. pylori*-associated GC, the correlation between tumor characteristics and each module was examined. As shown in Figure 3(e), among the 66 modules, modules light cyan, plum2, black, and magenta4 were most associated with stage (T_3 , T_2 , and T_4) with P values below 0.05; modules orangered4, salmon2, pink, and navajowhite2 were associated with lymph node metastasis (N_3 , N_2 , and N_0) were most correlated with P values below 0.05. We calculated MM and defined genes with $MM \geq 0.8$ as central genes among the genes in selected modules and obtained a total of 318 hub genes. The protein interaction networks of these 318 hub genes in their respective categories are shown in Figure 4.

3.5. Acquisition and Specificity Analysis of Key Genes. Seven genes obtained by intersecting the differential genes and hub genes were defined as key genes, namely, ADAM28, FCER1G, MRPL14, SOSTDC1, TYROBP, C1QC, and C3 (Figure 5(a)). Their expression in the tissues of the GSE13195 dataset is shown in Figure 5(b). Among them, FCER1G, MRPL14, TYROBP, C1QC, and C3 were significantly highly expressed in *H. pylori*-associated GC tissues compared with normal tissues, while ADAM28 and SOSTDC1 were completely opposite. In addition, the ROC curves showed that the key genes were well predicted (AUC values: 0.957, 0.902, 0.934, 0.925, 0.862, 0.826, and 0.726, respectively) (Figure 5(c)). This suggested that seven key genes had the potential to be diagnostic markers for *H. pylori*-associated GC.

3.6. Validation and Survival Analysis of Key Genes. Based on the TCGA database, boxplots of tumor samples and normal samples (including 34 normal samples, 20 *H. pylori*-associated GC samples, 157 *H. pylori*-unassociated GC samples, and 153 other samples) were generated for further validation of the key genes. As shown in Figure 6(a), the mRNA expression levels of the five key genes (FCER1G, MRPL14, C3, SOSTDC1, and TYROBP) were significantly different between tumor tissues and normal tissues, while ADAM28 and C1QC showed no significant differences. In addition, FCER1G, MRPL14, and C3 were abnormally high in *H. pylori*-associated and *H. pylori*-unassociated GC tissues compared to normal tissues; SOSTDC1 was abnormally low in *H. pylori*-associated and *H. pylori*-unassociated GC tissues. Interestingly, TYROBP was abnormally high in *H. pylori*-associated GC tissues compared to normal tissues but not in *H. pylori*-unassociated GC tissues. Furthermore, the expression of TYROBP was significantly increased in *H. pylori*-associated GC tissues relative to *H. pylori*-unassociated GC tissues. The expression levels of key genes were correlated with the prognosis of GC patients through survival analysis. According to the median expression value, GC patients were divided into a high expression group and low expression group. We found that patients with GC who

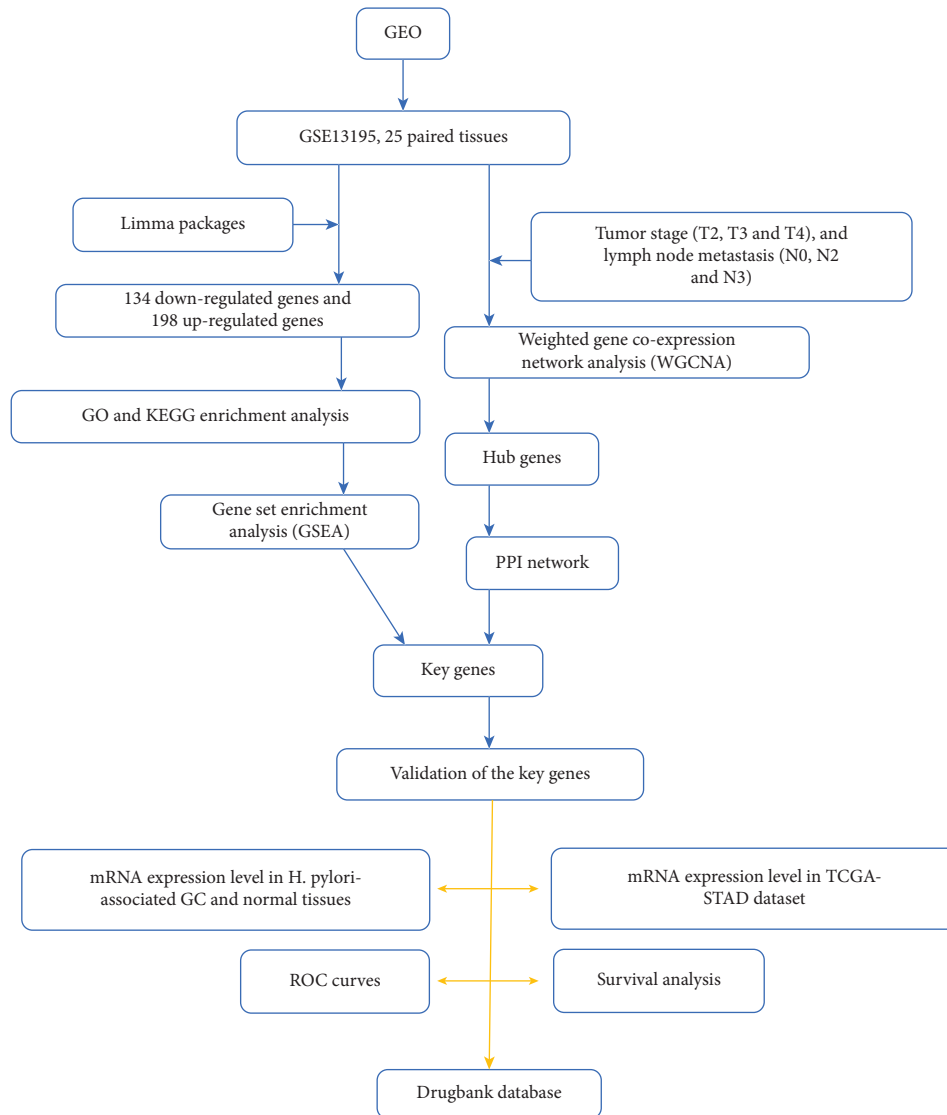


FIGURE 1: Flowchart of the study. GO: Gene Ontology; KEGG: Kyoto Encyclopedia of Genes and Genomes.

expressed high levels of C3 had poorer overall survival, while the results of survival analysis of other genes were not statistically significant (Figures 6(b) and S1). Therefore, we removed ADAM28 and C1QC from the key genes.

3.7. Immune Infiltration Analysis. We performed immune microenvironment analysis on *H. pylori*-associated GC and normal tissues according to the CIBERSORT's calculation method of the immune microenvironment score. As shown in Figures 7(a) and 7(b), compared with normal tissues, *H. pylori*-associated GC tissues had stronger infiltration of activated NK cells, M0 macrophages, M1 macrophages, and M2 macrophages, but less infiltration of plasma cells and CD8 T cells, others are no different. We used ssGSEA to determine enrichment scores for immune-related cells. Spearman correlations

between gene expression and immune enrichment scores for each hub were calculated and tested (Figure 7(c)). The results showed that FCER1G positively correlated with the infiltration of M2 macrophages, M1 macrophages, resting mast cells and resting dendritic cells, and negatively correlated with the infiltration of plasma cells and CD8 T cells. MRPL14 positively correlated with infiltration of M1 macrophages, M2 macrophages, M0 macrophages and resting dendritic cells, and negatively correlated with infiltration of plasma cells, CD8 T cells, and memory B cells. SOSTDC1 positively correlated with infiltration of plasma cells and CD8 T cells, and negatively correlated with infiltration of M0 macrophages, M1 macrophages, M2 macrophages, and activated NK cells. TYROBP was positively correlated with M2 macrophages, M1 macrophages, resting mast cells, and delta gamma T cell infiltration, and negatively correlated with

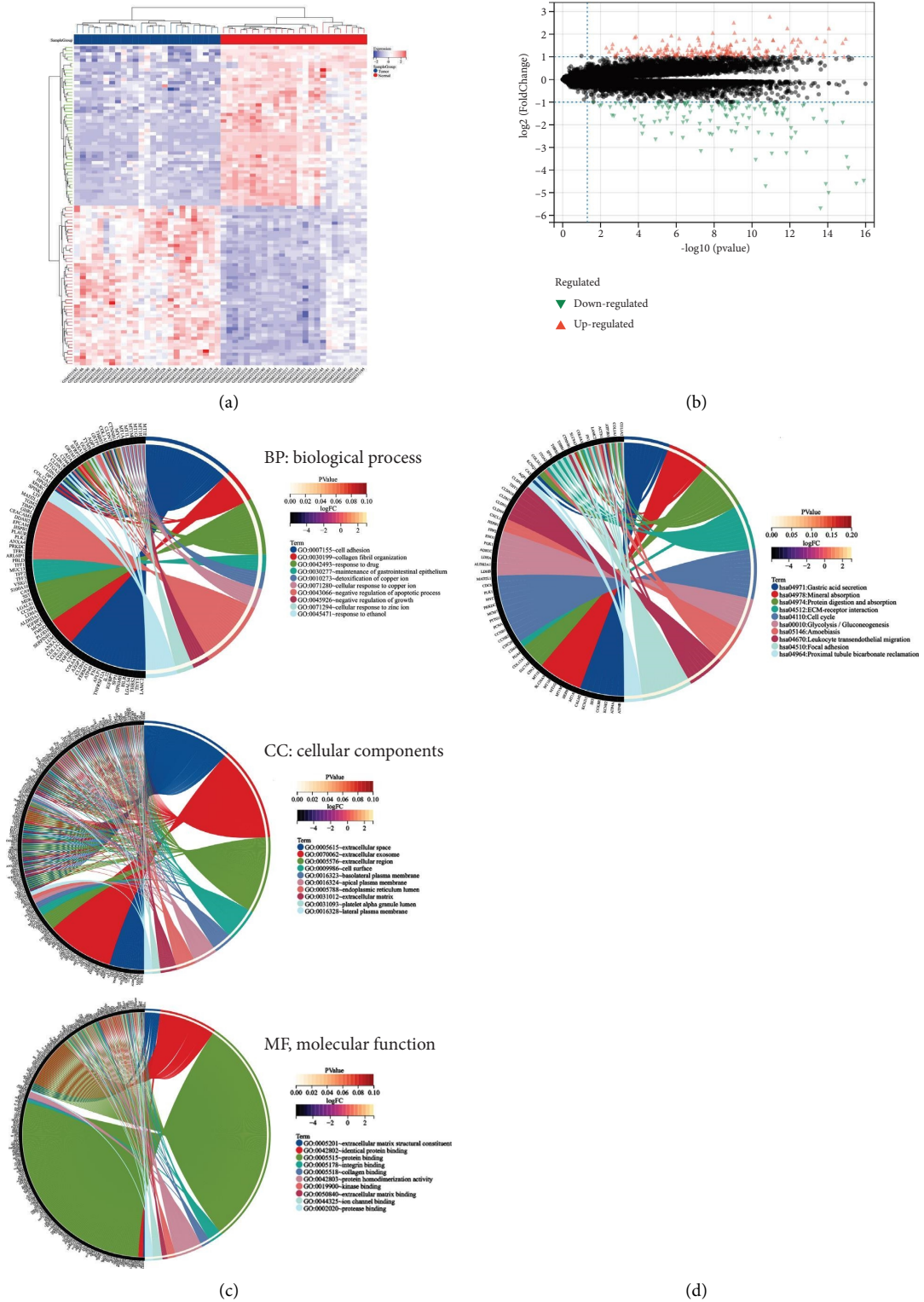
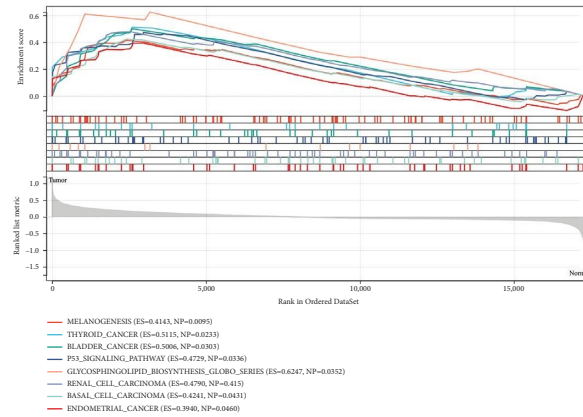


FIGURE 2: Continued.



(e)

FIGURE 2: The analysis of differentially expressed genes. (a) Heatmap of differentially expressed genes. (b) Volcano map of differential expressed genes. (c) Gene ontology (GO) enrichment analysis (top 10). (d) Kyoto Encyclopedia of Genes and Genomes (KEGG) pathway enrichment analysis (top 10). (e) Gene set enrichment analysis.

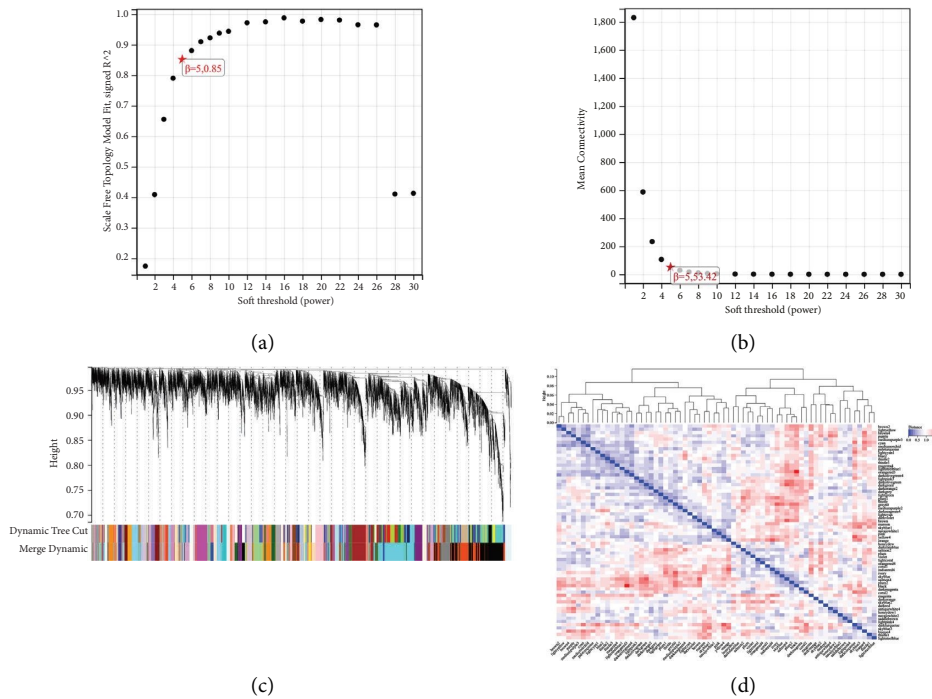


FIGURE 3: Continued.

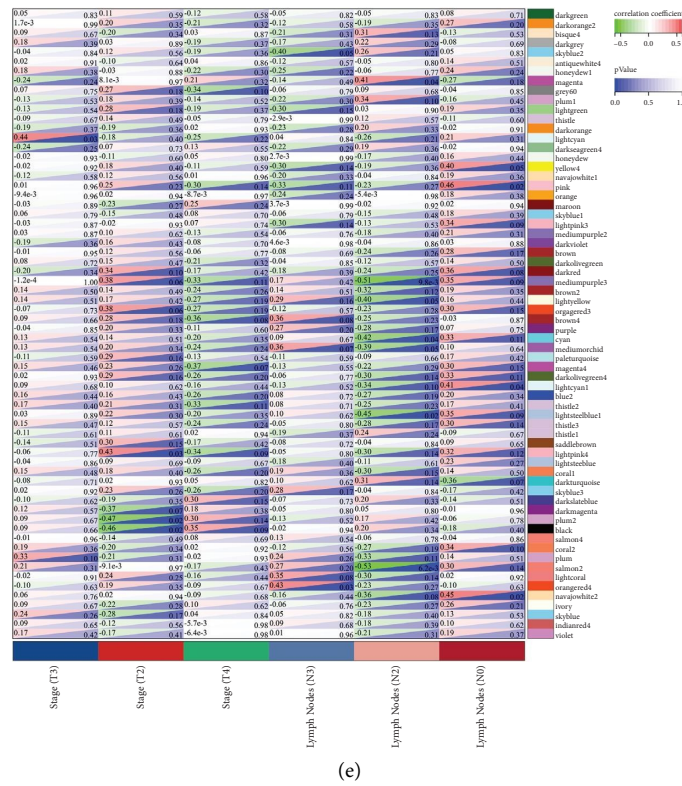


FIGURE 3: The weighted gene co-expression network analysis (WGCNA). (a) Analysis of the scale-free fit index for various soft-thresholding powers. (b) Analysis of the mean connectivity for various soft-thresholding powers. (c) Clustering dendrograms of GSE13195. (d) Module relationships. (e) Heat maps of the correlation between eigen gene and clinical traits of *H. pylori*-associated GC. GC: gastric cancer.

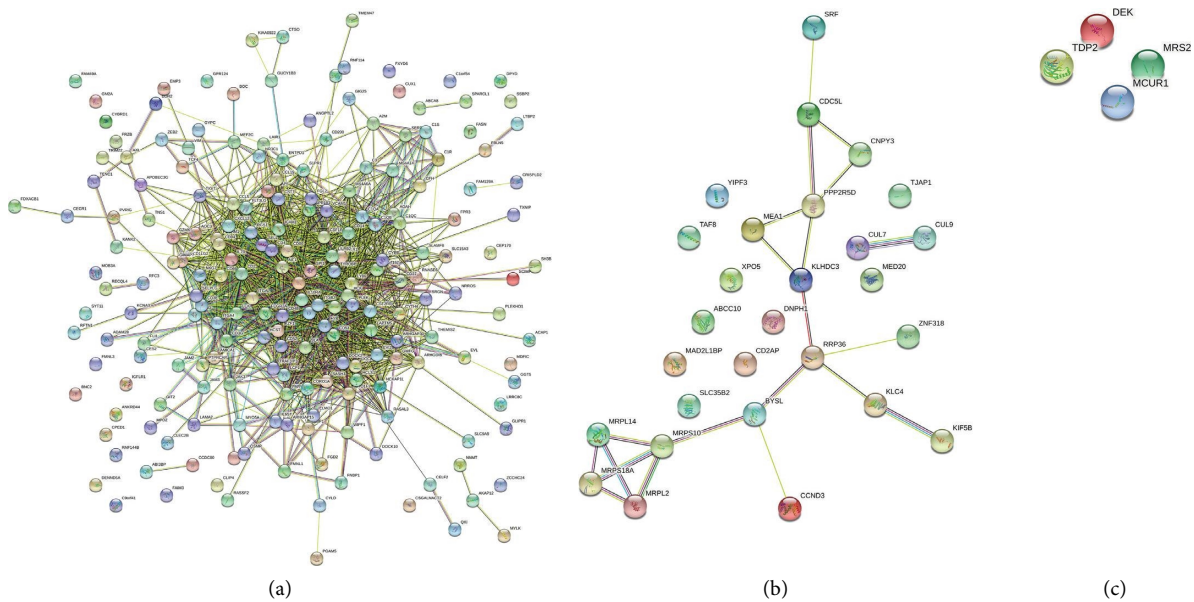


FIGURE 4: Continued.

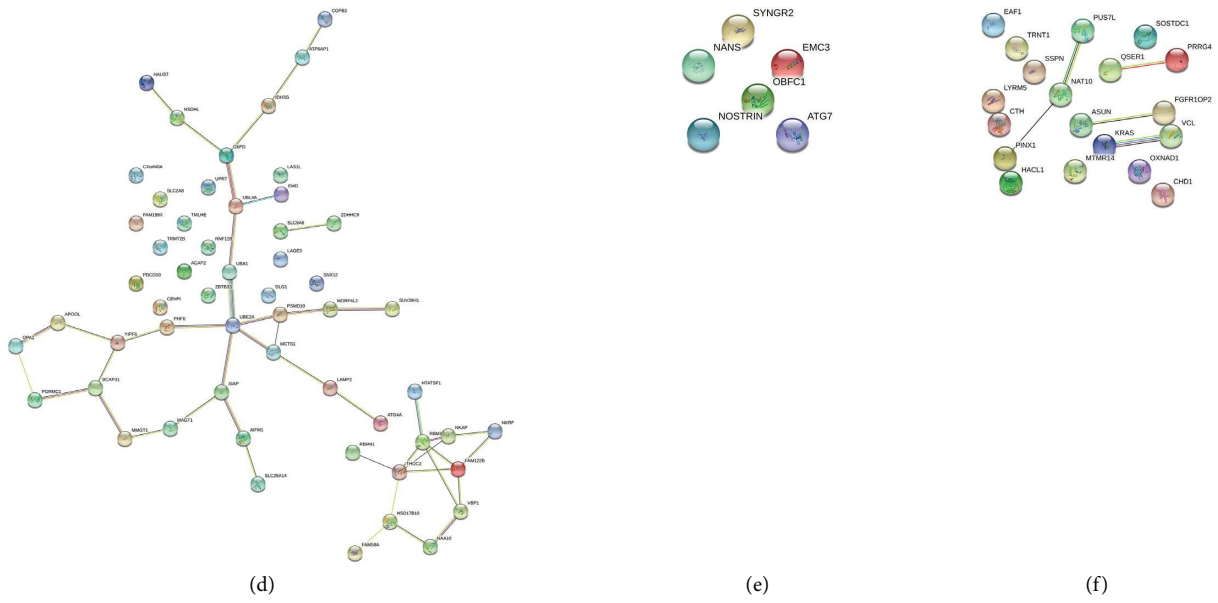


FIGURE 4: Protein-protein interaction (PPI) networks. (a) T3-related hub genes. (b) T2-related hub genes. (c) T4-related hub genes. (d) N3-related hub genes. (e) N2-related hub genes. (f) N0-related hub genes.

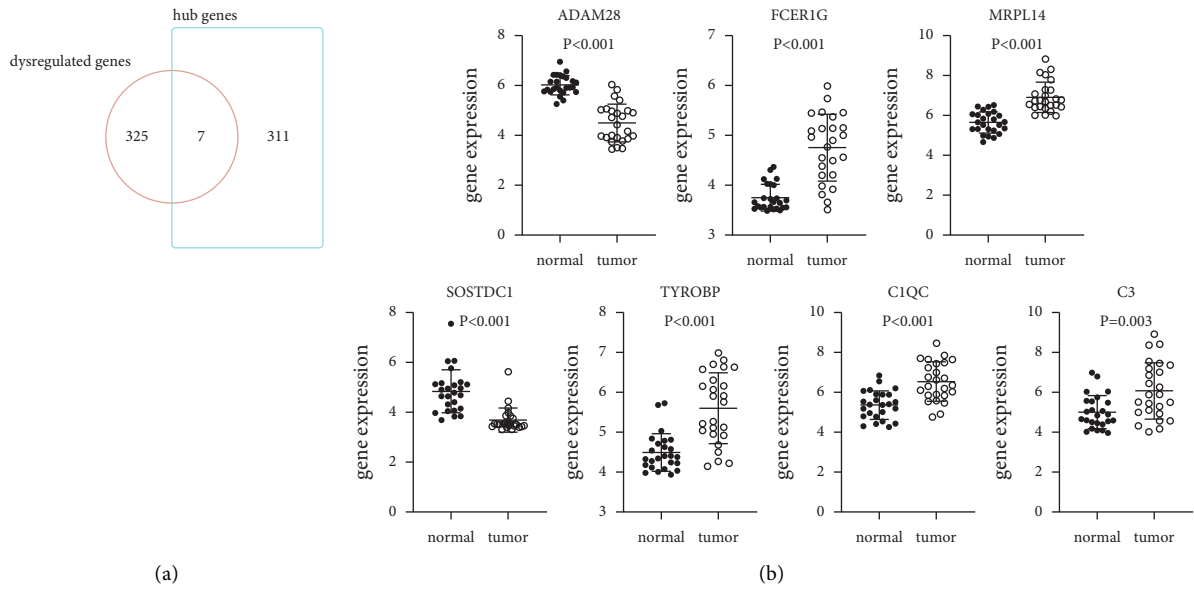


FIGURE 5: Continued.

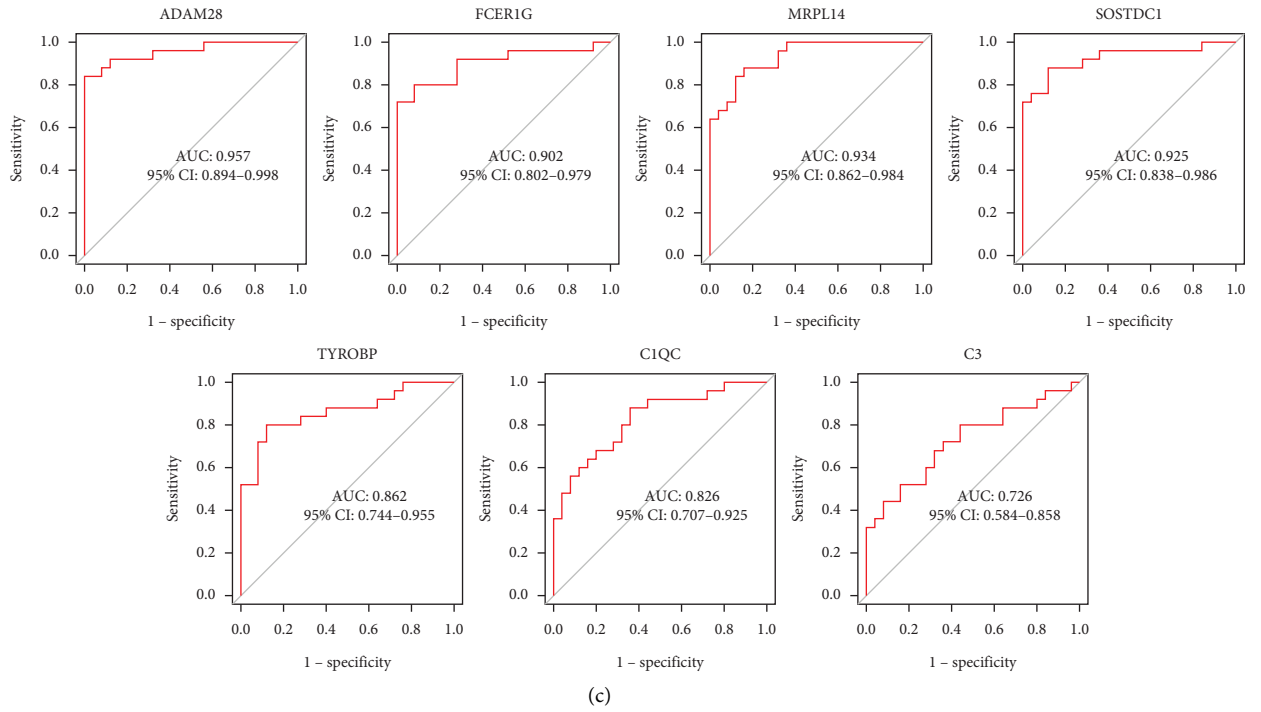


FIGURE 5: Validation of key genes in GSE13195. (a) Venn diagram. (b) mRNA expressions of key genes in GSE13195. (c) ROC curves of key genes in the diagnosis of *H. pylori*-associated GC. ROC: receiver operating characteristic. GC: gastric cancer.

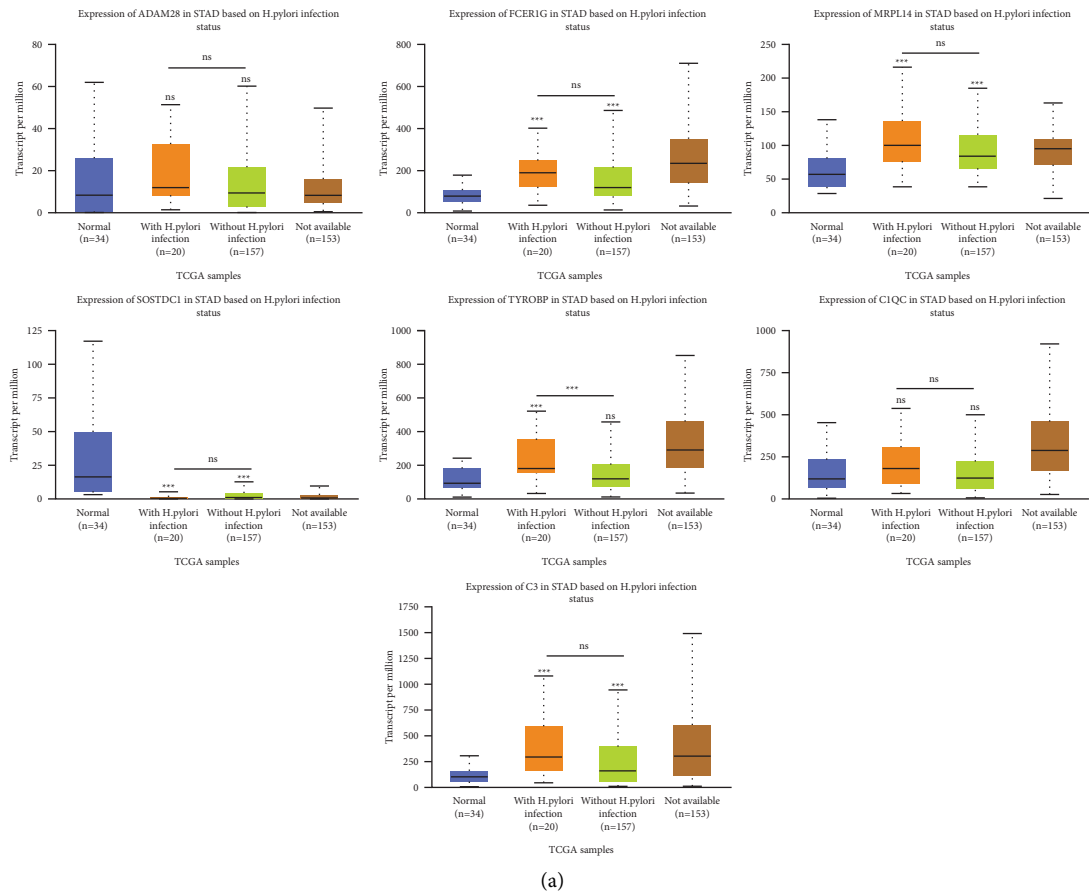
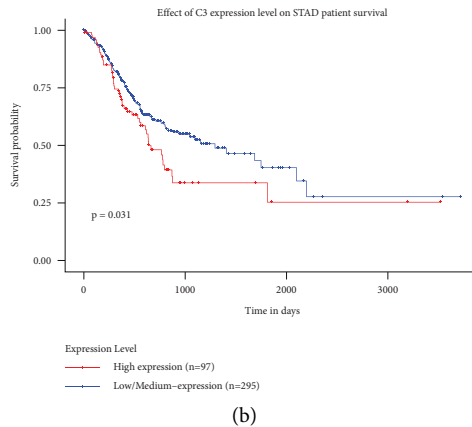
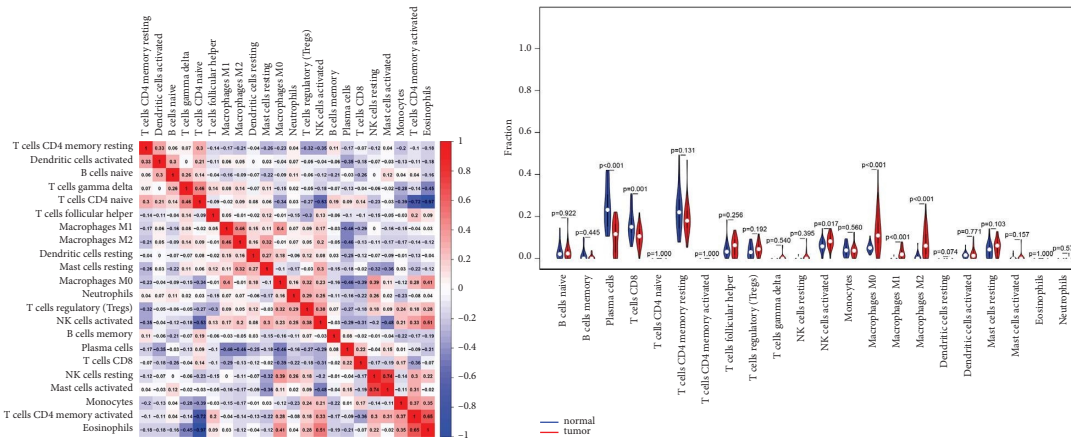


FIGURE 6: Continued.

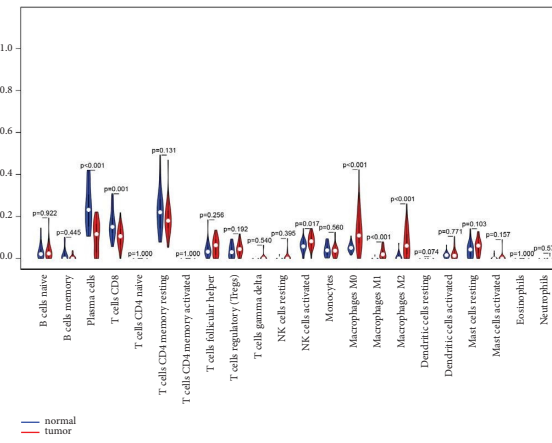


(b)

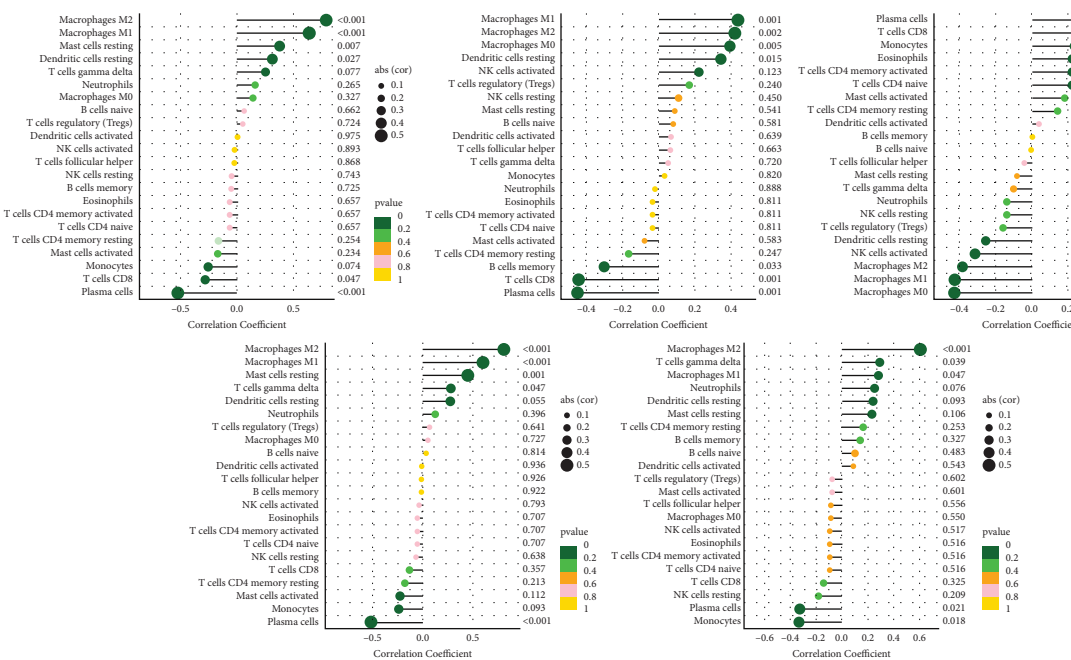
FIGURE 6: Validation of key genes in TCGA-STAD. (a) mRNA expressions of key genes in TCGA-STAD. (b) Association of C3 gene with overall survival of patients with GC.



(a)



(b)



(c)

FIGURE 7: Immune infiltration analysis. The color means spearman correlation between the hub gene and the immune-related cell. (a) Correlation matrix of all 22 immune cells proportions. (b) Violin plot showed the proportions of 22 immune cells between normal tissues with *H. pylori*-associated GC tissues. (c) Influence of key genes on infiltration of 22 immune cells.

plasma cell infiltration. C3 was positively correlated with infiltration of *M2* macrophages, delta gamma *T* cells and *M1* macrophages, and negatively correlated with infiltration of monocytes and plasma cells.

3.8. Possible Targeted Drugs. We used the DrugBank online website to search for possible targeted drugs in key genes. As shown in Table 1, for FCER1G, currently approved and under investigation drugs were benzylpenicilloyl polylysine and fostamatinib. Among them, benzylpenicilloyl polylysine acted as an agonist, while fostamatinib functioned as an inhibitor. For TYROBP, the currently approved and understudied drug was dasatinib, but it played a multi-targeted role, and the specific mechanism remained to be further studied. The remaining compounds targeting key genes were poorly studied.

4. Discussion

Globally, GC is the third most common malignancy as well as the sixth most common cause of death [1]. The recent research showed that more than half of newly diagnosed patients were from developing countries (Eastern Europe, East Asia, and Central and South America) [22]. GC can occur due to a number of risk factors, including exposure to chemical carcinogens, environmental factors, genetic susceptibility, poor diet, and excessive alcohol intake [23]. However, infection with *H. pylori* remains the main cause of GC induction [24]. Despite the rapid development of targeted therapies and immunotherapies in recent years, there was still a lack of clinical effectiveness in treating some patients with GC [25]. It would be beneficial if more methods and targets could be found for treating GC. Based on transcriptome data analysis, our study identified DEGs associated with the occurrence and progression of *H. pylori*-associated GC, and provided some potential targets for the treatment of *H. pylori*-associated GC. Based on the GSE13195 and TCGA-STAD datasets, we identified five key genes, FCER1G, MRPL14, SOSTDC1, TYROBP, and C3, which presented different expression patterns in *H. pylori*-associated GC and normal tissues, where C3 may affect the prognosis of GC patients.

FCER1G is located on chromosome 1q23.3 and encodes the gamma subunit of the crystalline (Fc) region (Fc R) of an immunoglobulin fragment involved in various immune responses such as phagocytosis and cytokine release [26, 27]. Cellular effector functions are activated by the interaction between the Fc of immunoglobulins and the Fc R of immune cells, which in turn trigger destructive inflammation, immune cell activation, phagocytosis, oxidative burst, and cytokine release [28, 29]. FCER1G was implicated in the progression of several cancers, such as squamous cell carcinoma, multiple myeloma, and clear cell renal cell carcinoma [27, 29, 30]. In renal cancer, the high expression of FCER1G may be a functional basis for the induction of *M2* macrophages by the increased secretion of IL-4. In addition,

M2 macrophages can acquire their tumor suppressor function in part by suppressing cytotoxic *T* cells. This may explain the relevance of FCER1G to macrophage and *T* cell function [31]. These findings were consistent with our results that high expression of FCER1G was positively correlated with infiltration of *M2* macrophages and negatively correlated with CD8 *T* cells.

MRPL14 is a highly conserved protein. One protein-binding site and two RNA-binding sites are located in the C-terminal region of MRPL14, which consists of a five-stranded beta barrel and two small alpha helices [32]. MRPL14 was found to be closely related to mitochondrial metabolism [33]. The conserved interaction of C7orf30 with MRPL14 promoted biogenesis of the mitochondrial large ribosomal subunit and mitochondrial translation [32]. However, research on the role of MRPL14 in cancers is currently still blank.

SOSTDC1 is a secreted protein with a glycosylated N-terminus that contains a C-terminal cysteine knot domain [34]. SOSTDC1 negatively regulates BMP (bone morphogenetic protein) signaling during cell proliferation, differentiation, and apoptosis, and also regulates various processes in development and cancer by regulating the Wnt pathway [35, 36]. Researchers have found that a lack of SOSTDC1 in GC patients was associated with a shorter survival rate. In gastric cancer, SOSTDC1 acts like a tumor suppressor, and its silencing can promote tumor growth and lung metastasis. SOSTDC1 significantly inhibits the SMAD-dependent BMP pathway, c-Jun activation, and transcription of c-Jun downstream targets [37]. In addition, SOSTDC1 regulates NK cell maturation and Ly49 receptor expression from nonhematopoietic and hematopoietic sources in a cellular-exogenous manner [38]. This seems to be contrary to the results we obtained in *H. pylori*-associated GC tissues, which needs to be further explored in the follow-up studies.

TYROBP, also known as DAP12, can noncovalently bind to activating receptors on the surface of various immune cells and mediate signal transduction and cell activation [39, 40]. There was evidence that patients with GC who overexpressed TYROBP had a poorer survival rate. Furthermore, TYROBP can stimulate macrophage activation, regulate tumor necrosis factor production, and induce tolerance [41]. TYROBP is involved in the interaction between tumor cells and macrophage *M2* to enhance TGF- β secretion *in vitro* [42]. Our research partially confirmed this, but this part of the results still needs to be verified with large samples later.

Complement is an important part of the innate immune system. Previously, it was thought to be a network of proteins that released inflammatory mediators in response to microbial invasion [43]. A growing number of studies have shown that complement activation in the tumor microenvironment can delay local *T*-cell immunosuppression and chronic inflammation, thereby promoting tumor-promoting effects, ultimately promoting tumor immune escape, growth, and distant metastasis [44, 45]. C3 and downstream signaling molecules are involved in multiple biological processes of tumor cells, including tumor cell anchoring,

TABLE 1: Potential targeted drugs of key genes.

Genes	Potential drugs	Drug group	Actions
FCER1G	Benzylpenicilloyl polylysine	Approved	Agonist
	Fostamatinib	Approved, investigational	Inhibitor
TYROBP	Dasatinib	Approved, investigational	Multitarget

proliferation, tumor-associated angiogenesis, matrix remodeling, migration, and invasion [46–48]. In GC, monocytes, TAMs, M2 macrophages, DCs, Tregs, and T cell exhaustion were significantly associated with C3 expression. An immunotherapeutic approach based on C3 could provide a potential biological target for GC [49].

Although we identified and confirmed 5 key genes that were highly correlated with the progression of *H. pylori*-associated GC, we were unable to perform multifaceted validation due to the small sample size of GSE13195 and the lack of studies of the same type. In addition, we did not perform experimental tests on key genes. It is critical to conduct larger sample studies as well as multicenter clinical trials to gain a deeper understanding of how genes are involved in *H. pylori*-associated gastric cancer.

5. Conclusion

In conclusion, we identified five key genes, FCER1G, MRPL14, SOSTDC1, TYROBP, and C3, associated with the occurrence of GC in *H. pylori* infection. Among them, *H. pylori*-associated GC patients with higher C3 expression had worse prognosis than those with lower expression. In addition, in the future, *H. pylori*-associated GC may be diagnosed and treated precisely by biomarkers and therapeutic targets related to these key genes.

Data Availability

The datasets used and/or analyzed during the current study are available from the corresponding author upon reasonable request.

Conflicts of Interest

The authors declare that they have no conflicts of interest.

Authors' Contributions

DW and TY conceived and designed the project; DW, ZL, and YZP acquired the data; DW, XWB, and XXZ analyzed and interpreted the data; DW, JH, and YN wrote the paper. All authors contributed to the study and approved the submitted version. Wei Ding, Huaji Jiang, and Nianyuan Ye contributed equally to this work.

Acknowledgments

This work was supported by the Changzhou Sci & Tech Program (Nos. CJ20210013 and CJ20220008), Young Talent Development Plan of Changzhou Health Commission (Nos. CZQM2020118 and CZQM2021028), the Development Foundation of Affiliated Hospital of Xuzhou Medical

University (No. XYFY2020016), Medical Research Project of Jiangsu Health Commission (No. Z2019027), and Changzhou High-Level Medical Talents Training Project (No. 2022CZBJ105).

Supplementary Materials

Figure S1. Association of ADAM28, FCER1G, MRO14, SOSTDC1, TYROBP, and C1QC genes with overall survival of patients with GC. (*Supplementary Materials*)

References

- [1] H. Sung, J. Ferlay, R. L. Siegel et al., “Global cancer statistics 2020: GLOBOCAN estimates of incidence and mortality worldwide for 36 cancers in 185 countries,” *CA: A Cancer Journal for Clinicians*, vol. 71, no. 3, pp. 209–249, 2021.
- [2] W. Chen, R. Zheng, P. D. Baade et al., “Cancer statistics in China, 2015,” *CA: A Cancer Journal for Clinicians*, vol. 66, no. 2, pp. 115–132, 2016.
- [3] A. Högnér and M. Moehler, “Immunotherapy in gastric cancer,” *Current Oncology*, vol. 29, no. 3, pp. 1559–1574, 2022.
- [4] F. M. Johnston and M. Beckman, “Updates on management of gastric cancer,” *Current Oncology Reports*, vol. 21, no. 8, p. 67, 2019.
- [5] E. C. Smyth, M. Nilsson, H. I. Grabsch, N. C. van Grieken, and F. Lordick, “Gastric cancer,” *The Lancet*, vol. 396, no. 10251, pp. 635–648, 2020.
- [6] E. A. Ashley, “The precision medicine initiative: a new national effort,” *JAMA*, vol. 313, no. 21, pp. 2119–2120, 2015.
- [7] J. Matsuzaki, H. Tsugawa, and H. Suzuki, “Precision medicine approaches to prevent gastric cancer,” *Gut and Liver*, vol. 15, no. 1, pp. 3–12, 2021.
- [8] A. O’Connor, C. A. O’Morain, and A. C. Ford, “Population screening and treatment of *Helicobacter pylori* infection,” *Nature Reviews Gastroenterology & Hepatology*, vol. 14, no. 4, pp. 230–240, 2017.
- [9] A. C. Ford, Y. Yuan, and P. Moayyedi, “*Helicobacter pylori* eradication therapy to prevent gastric cancer: systematic review and meta-analysis,” *Gut*, vol. 69, no. 12, pp. 2113–2121, 2020.
- [10] R. M. Peek Jr. and J. E. Crabtree, “*Helicobacter* infection and gastric neoplasia,” *The Journal of Pathology*, vol. 208, no. 2, pp. 233–248, 2006.
- [11] P. Correa, “Human gastric carcinogenesis: a multistep and multifactorial process--first American cancer society award lecture on cancer epidemiology and prevention,” *Cancer Research*, vol. 52, no. 24, pp. 6735–6740, 1992.
- [12] M. J. Blaser and J. C. Atherton, “*Helicobacter pylori* persistence: biology and disease,” *Journal of Clinical Investigation*, vol. 113, no. 3, pp. 321–333, 2004.
- [13] R. Zappasodi, T. Merghoub, and J. D. Wolchok, “Emerging concepts for immune checkpoint blockade-based combination therapies,” *Cancer Cell*, vol. 34, no. 4, p. 690, 2018.
- [14] T. Wu and Y. Dai, “Tumor microenvironment and therapeutic response,” *Cancer Letters*, vol. 387, pp. 61–68, 2017.

- [15] E. Clough and T. Barrett, "The gene expression Omnibus database," *Methods in Molecular Biology*, vol. 1418, pp. 93–110, 2016.
- [16] W. Shen, Z. Song, X. Zhong et al., "Sangerbox: a comprehensive, interaction-friendly clinical bioinformatics analysis platform," *iMeta*, vol. 1, no. 3, p. e36, 2022.
- [17] B. T. Sherman, M. Hao, J. Qiu et al., "DAVID: a web server for functional enrichment analysis and functional annotation of gene lists (2021 update)," *Nucleic Acids Research*, vol. 50, no. 1, pp. W216–W221, 2022.
- [18] P. Langfelder and S. Horvath, "WGCNA: an R package for weighted correlation network analysis," *BMC Bioinformatics*, vol. 9, no. 1, p. 559, 2008.
- [19] D. S. Chandrashekar, S. K. Karthikeyan, P. K. Korla et al., "UALCAN: an update to the integrated cancer data analysis platform," *Neoplasia*, vol. 25, pp. 18–27, 2022.
- [20] B. Chen, M. S. Khodadoust, C. L. Liu, A. M. Newman, and A. A. Alizadeh, "Profiling tumor infiltrating immune cells with CIBERSORT," *Methods in Molecular Biology*, vol. 1711, pp. 243–259, 2018.
- [21] D. S. Wishart, C. Knox, A. C. Guo, S. Shrivastava, M. Hassanali, and P. Stothard, "DrugBank: a comprehensive resource for in silico drug discovery and exploration," *Nucleic Acids Research*, vol. 34, no. 90001, pp. D668–D672, 2006.
- [22] M. Tyczyńska, P. Kędzierawski, K. Karakuła et al., "Treatment strategies of gastric cancer-molecular targets for anti-angiogenic therapy: a state-of-the-art review," *Journal of Gastrointestinal Cancer*, vol. 52, no. 2, pp. 476–488, 2021.
- [23] J. Baj, A. Forma, M. Sitarz et al., "*Helicobacter pylori* virulence factors-mechanisms of bacterial pathogenicity in the gastric microenvironment," *Cells*, vol. 10, no. 1, p. 27, 2020.
- [24] M. Puculek, J. Machlowska, R. Wierzbicki, J. Baj, R. Maciejewski, and R. Sitarz, "*Helicobacter pylori* associated factors in the development of gastric cancer with special reference to the early-onset subtype," *Oncotarget*, vol. 9, no. 57, pp. 31146–31162, 2018.
- [25] S. S. Joshi and B. D. Badgwell, "Current treatment and recent progress in gastric cancer," *CA: A Cancer Journal for Clinicians*, vol. 71, no. 3, pp. 264–279, 2021.
- [26] M. Tsuji, Y. Ezumi, M. Arai, and H. Takayama, "A novel association of Fc receptor gamma-chain with glycoprotein VI and their co-expression as a collagen receptor in human platelets," *Journal of Biological Chemistry*, vol. 272, no. 38, pp. 23528–23531, 1997.
- [27] L. Fu, Z. Cheng, F. Dong et al., "Enhanced expression of FCER1G predicts positive prognosis in multiple myeloma," *Journal of Cancer*, vol. 11, no. 5, pp. 1182–1194, 2020.
- [28] P. Andreu, M. Johansson, N. I. Affara et al., "FcRγ activation regulates inflammation-associated squamous carcinogenesis," *Cancer Cell*, vol. 17, no. 2, pp. 121–134, 2010.
- [29] S. Kraft and J. P. Kinet, "New developments in FcεRI regulation, function and inhibition," *Nature Reviews Immunology*, vol. 7, no. 5, pp. 365–378, 2007.
- [30] L. Chen, L. Yuan, Y. Wang et al., "Co-expression network analysis identified FCER1G in association with progression and prognosis in human clear cell renal cell carcinoma," *International Journal of Biological Sciences*, vol. 13, no. 11, pp. 1361–1372, 2017.
- [31] K. Dong, W. Chen, X. Pan et al., "FCER1G positively relates to macrophage infiltration in clear cell renal cell carcinoma and contributes to unfavorable prognosis by regulating tumor immunity," *BMC Cancer*, vol. 22, no. 1, p. 140, 2022.
- [32] S. Fung, T. Nishimura, F. Sasarman, and E. A. Shoubridge, "The conserved interaction of C7orf30 with MRPL14 promotes biogenesis of the mitochondrial large ribosomal subunit and mitochondrial translation," *Molecular Biology of the Cell*, vol. 24, no. 3, pp. 184–193, 2013.
- [33] C. Jacques, D. Guillotin, J. F. Fontaine et al., "DNA microarray and miRNA analyses reinforce the classification of follicular thyroid tumors," *Journal of Clinical Endocrinology and Metabolism*, vol. 98, no. 5, pp. E981–E989, 2013.
- [34] M. Yanagita, "BMP antagonists: their roles in development and involvement in pathophysiology," *Cytokine & Growth Factor Reviews*, vol. 16, no. 3, pp. 309–317, 2005.
- [35] M. Yanagita, M. Oka, T. Watabe et al., "USAG-1: a bone morphogenetic protein antagonist abundantly expressed in the kidney," *Biochemical and Biophysical Research Communications*, vol. 316, no. 2, pp. 490–500, 2004.
- [36] K. B. Lintern, S. Guidato, A. Rowe, J. W. Saldanha, and N. Itasaki, "Characterization of wise protein and its molecular mechanism to interact with both Wnt and BMP signals," *Journal of Biological Chemistry*, vol. 284, no. 34, pp. 23159–23168, 2009.
- [37] R. A. Bartolomé, L. Pintado-Berninches, M. Jaén, V. de Los Ríos, J. I. Imbaud, and J. I. Casal, "SOSTDC1 promotes invasion and liver metastasis in colorectal cancer via interaction with ALCAM/CD166," *Oncogene*, vol. 39, no. 38, pp. 6085–6098, 2020.
- [38] A. J. Millan, S. R. Elizaldi, E. M. Lee et al., "Sostdc1 regulates NK cell maturation and cytotoxicity," *The Journal of Immunology*, vol. 202, no. 8, pp. 2296–2306, 2019.
- [39] L. L. Lanier, B. Corliss, J. Wu, and J. H. Phillips, "Association of DAP12 with activating CD94/NKG2C NK cell receptors," *Immunity*, vol. 8, no. 6, pp. 693–701, 1998.
- [40] J. Dietrich, M. Cella, M. Seiffert, H. J. Bühring, and M. Colonna, "Cutting edge: signal-regulatory protein beta 1 is a DAP12-associated activating receptor expressed in myeloid cells," *The Journal of Immunology*, vol. 164, no. 1, pp. 9–12, 2000.
- [41] J. Jiang, Y. Ding, M. Wu et al., "Identification of TYROBP and CIQB as two novel key genes with prognostic value in gastric cancer by network analysis," *Frontiers Oncology*, vol. 10, p. 1765, 2020.
- [42] R. Takamiya, K. Ohtsubo, S. Takamatsu, N. Taniguchi, and T. Angata, "The interaction between Siglec-15 and tumor-associated sialyl-Tn antigen enhances TGF-β secretion from monocytes/macrophages through the DAP12-Syk pathway," *Glycobiology*, vol. 23, no. 2, pp. 178–187, 2013.
- [43] D. Ricklin, G. Hajishengallis, K. Yang, and J. D. Lambris, "Complement: a key system for immune surveillance and homeostasis," *Nature Immunology*, vol. 11, no. 9, pp. 785–797, 2010.
- [44] M. M. Markiewski, R. A. DeAngelis, F. Benencia et al., "Modulation of the antitumor immune response by complement," *Nature Immunology*, vol. 9, no. 11, pp. 1225–1235, 2008.
- [45] E. Bonavita, S. Gentile, M. Rubino et al., "PTX3 is an extrinsic oncosuppressor regulating complement-dependent inflammation in cancer," *Cell*, vol. 160, no. 4, pp. 700–714, 2015.
- [46] R. Pio, L. Corrales, and J. D. Lambris, "The role of complement in tumor growth," *Advances in Experimental Medicine and Biology*, vol. 772, pp. 229–262, 2014.
- [47] D. Ajona, S. Ortiz-Espinosa, and R. Pio, "Complement anaphylatoxins C3a and C5a: emerging roles in cancer

- progression and treatment,” *Seminars in Cell & Developmental Biology*, vol. 85, pp. 153–163, 2019.
- [48] E. S. Reis, D. C. Mastellos, D. Ricklin, A. Mantovani, and J. D. Lambris, “Complement in cancer: untangling an intricate relationship,” *Nature Reviews Immunology*, vol. 18, no. 1, pp. 5–18, 2018.
- [49] D. Bao, C. Zhang, L. Li et al., “Integrative analysis of complement system to prognosis and immune infiltrating in colon cancer and gastric cancer,” *Frontiers Oncology*, vol. 10, p. 553297, 2020.